Bioconjugate Chemistry

Article

pubs.acs.org/bc

Rapid Synthesis of Cyclic RGD Conjugated Gold Nanoclusters for Targeting and Fluorescence Imaging of Melanoma A375 Cells

Hua-Qin Yin, Feng-Li Bi, and Feng Gan*

School of Chemistry and Chemical Engineering, Sun Yat-Sen University, Guangzhou 510275, P.R. China

Supporting Information

ABSTRACT: A simple, rapid, and inexpensive method for the synthesis of cyclic arginine-glycine-aspartic acid (RGD) peptide conjugated gold nanoclusters (RGD-GNCs) was reported. The nanoclusters were synthesized with chlorаurate as precursor and cyclic RGD peptides as both reducing and protecting agent directly under alkali condition, and the whole synthetic process only took 15 min at room temperature. The properties of the nanoclusters were characterized by means of ultraviolet−visible spectra, Fourier transform infrared spectroscopy (FTIR), fluorescence, transmission electron microscopy (TEM), and X-ray photoelectron spectroscopy (XPS). The prepared gold nanoclusters were successfully used as a contrast agent in fluorescence imaging of the melanoma A375 cells, which overexpress the integrin $\alpha_v\beta_3$. The results demonstrated that our nanoclusters possess good biocompatibility, stability, and low toxicity. Moreover, the method is expected to be applicable to the synthesis of nanoclusters conjugated with other biomolecules.

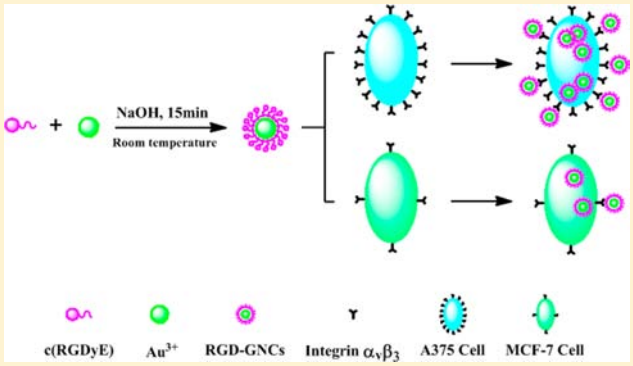

INTRODUCTION

Peptides containing the arginine-glycine-aspartic acid (RGD) sequence have been receiving extensive attention recently because they can recognize the integrin $\alpha_v\beta_3$ that is highly expressed by several solid tumors, such as melanomas,[1] ovarian cancers,[2] and glioblastomas.[3] To date, many kinds of RGD peptide conjugated nanomaterials, such as silicon nanomaterials,[4] quantum dots,[5,6] and metal nanoparticles,[7−11] were reported to perform the tumor targeted therapy and imaging. Among these nanomaterials, gold nanomaterials are especially recommended due to their good chemical and optical properties, good biocompatibility, and low toxicity. RGD conjugated gold nanoparticles (GNPs) have been synthesized and used as contrast agents in tumor imaging.[7−10] Compared with GNPs, gold nanoclusters (GNCs) have been recognized as more promising candidates for tumor therapy and imaging because of their ultrasmall size, molecular-like properties, luminescence, and unique charging properties.[12] The common method to synthesis GNCs uses sodium borohydride as reducing agent and the derivatives containng amine or thiol groups as protecting agent. In 2009, Ying et al.[13] reported a simple and "green" synthetic route to prepare GNCs using bovine serum albumin (BSA) as reducing and stabilizing agent. One year later, Lee et al.[14] discovered that the reduction capability of a peptide depends on the presence of certain reducing amino acid residues. The work from these two groups inspired many researchers who used proteins, such as lysozyme,[15] insulin,[16] apoferritin,[17] and specific peptides,[18] as scaffolds for the preparation of GNCs.

In this paper, we report a simple, rapid, and inexpensive method for the synthesis of cyclic RGD peptide conjugated gold nanoclusters (RGD-GNCs), which is also a one-step method and only needs 15 min. In the synthesis process, we made RGD peptides act as both reducing and protecting agents. More importantly, the prepared RGD-GNCs possess good biocompatibility, stability, and low toxicity. The recognition between the RGD conjugated GNCs and the integrin $\alpha_v\beta_3$ was not noticeably influenced after the peptides acting as reducing reagent. The RGD-GNCs had been successfully used in the fluorescence imaging of the melanoma A375 cells.

RESULTS AND DISCUSSION

We observed that the order of addition of raw materials, the ratio of c(RGDyE)/$HAuCl_4$, pH, reaction time, and temperature had a strong influence on the synthesis reaction (see Supporting Information). If the gold ions were added into the mixed solution of NaOH and peptides, the fluorescence intensity would be larger than that with other additional orders (Supporting Information Figure S1), which demonstrated that the peptides' reducing activity was fully motivated in alkaline environment.[18] If we mixed NaOH with gold ions at first, no fluorescence increase was observed, which meant that most gold ions were converted to less reactive $[AuCl_2(OH)_2]^-$ and

Received: November 4, 2014
Revised: December 30, 2014
Published: January 15, 2015

DOI: 10.1021/bc500505c
Bioconjugate Chem. 2015, 26, 243−249

$[AuCl(OH)_3]^-$ (Supporting Information Figure S1).[19] Moreover, if the reaction solution was kept at room temperature for 10 min, green fluorescent GNCs appeared. The reaction efficiency was increased at higher temperature (Supporting Information Figure.S2). In this work, the reaction was kept at room temperature to maintain the biological stability of the peptides and the ease of operation. Interestingly, the green fluorescence of GNCs appeared in just 1 min under our optimized conditions, which indicated that the peptides' reducibility is strong enough to reduce gold ions into gold atoms that then joined in the generation of GNCs. The reaction time was set at 15 min (Supporting Information Figure S5) which is quite short compared with other reports that need at least 6 h.[13,15−18] The reason for other works might be that the proteins and peptides contain the cysteine (C), histidine (H), and methionine (M), which are known to form strong complexes with metal ions.[20] Generally, complexation lowers the redox potential and hence the reducibility of the metal ions. The results of the optimization processes were shown in Supporting Information (Figures S3 and S4).

In addition, we investigated the feasibility of c(RGDyE), c(RGDyC), c(RGDfC), c(RGDfV), and linear RGD tripeptide in the synthesis of the RGD-GNCs (Figure 1). As shown in

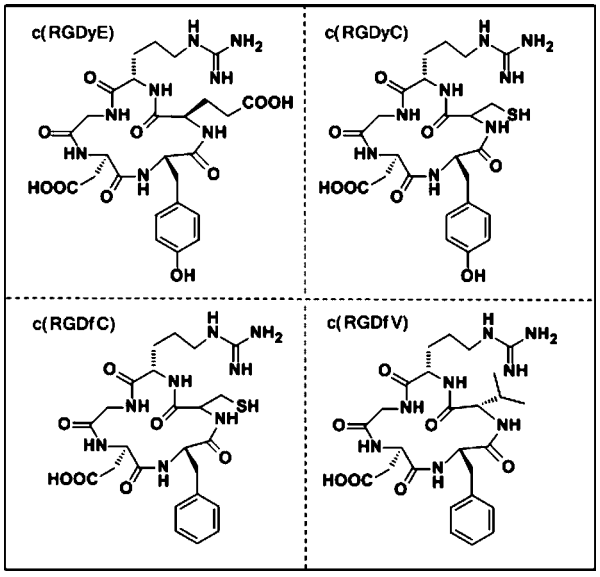

Figure 1. Cyclic peptides' sequences of c(RGDyE), c(RGDyC), c(RGDfC), and c(RGDfV).

Figure 2, only c(RGDyE) and c(RGDyC) could be used to prepare green GNCs. The reason could be that the tyrosine (y), the phenolic group of tyrosine of the cyclic peptides c(RGDyE) and c(RGDyC), can reduce gold ions into GNCs.[13,18] The fluorescence intensity of the c(RGDyE) products was much larger than that of the c(RGDyC) products, the reason possibly being that the c(RGDyE) possesses two carboxy groups which can stabilize colloidal solution under alkaline condition after the peptides conjugated onto the surface of GNCs,[21] although the gold ions can interact with the thiol group of cysteine (C). The reducibility of c(RGDfC) and c(RGDfV) was not strong enough because no fluorescent products were produced. Linear RGD peptides had been used to prepare gold nanoparticles[10] but failed to prepare GNCs because of their weak reducibility, and these results coincided with that of Lee's group.[14]

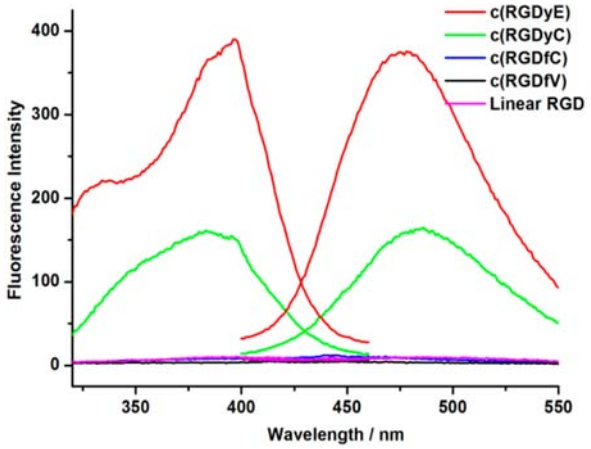

Figure 2. Fluorescence excitation and emission spectra of linear and cyclic RGD peptides prepared GNCs (excitation at 385 nm and emission at 485 nm).

In the sequence of c(RGDyE) peptides, the tyrosine (Tyr) residue have strong electron donating properties in situ reducing Au(III) ions to Au colloids.[13,14,22] The phenolic group of tyrosine of the cyclic peptides c(RGDyE) can reduce Au ions and then change into a phenoxide structure,[18] which is consistent with our result of UV−vis spectra as shown in Figure 3. The absorption peak at 274 nm of the pure c(RGDyE)

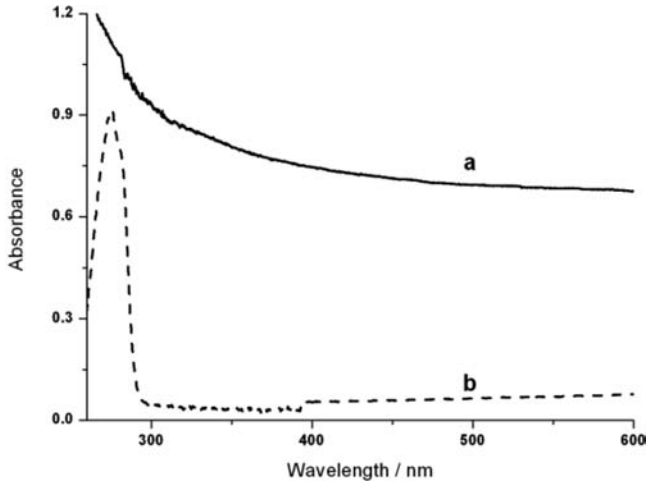

Figure 3. UV−visible absorption spectra of the as-prepared RGD-GNCs (a), and the cyclic peptides (b).

peptide, which comes from the tyrosine (y), disappeared in the spectra of dialyzed GNCs because the benzene of tyrosine was destroyed in the formation of a phenoxide structure while the phenolic group of tyrosine played a reducing role in the basic condition.[18]

The transmission electron microscopy (TEM) images (Figure 4) clearly proved that most of the GNCs were well dispersed and the average particle diameter was about 2.0 nm.

The emission band of the RGD-GNCs was approximately centered at 485 nm upon excitation at 385 nm (black curves in Figure 5). The inset shows that RGD-GNCs emitted a green fluorescence under UV light (365 nm), while c(RGDyE) and gold ions did not have any fluorescence under the same test condition (blue and red curves).

DOI: 10.1021/bc500505c
Bioconjugate Chem. 2015, 26, 243−249

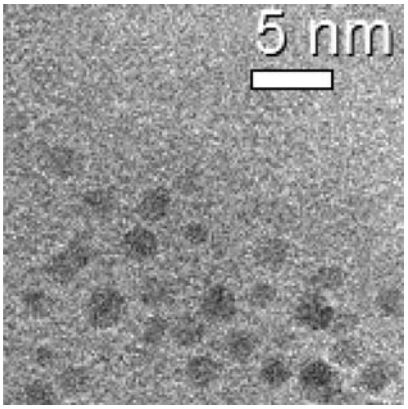

Figure 4. TEM image of RGD-GNCs. Scale bar 5 nm.

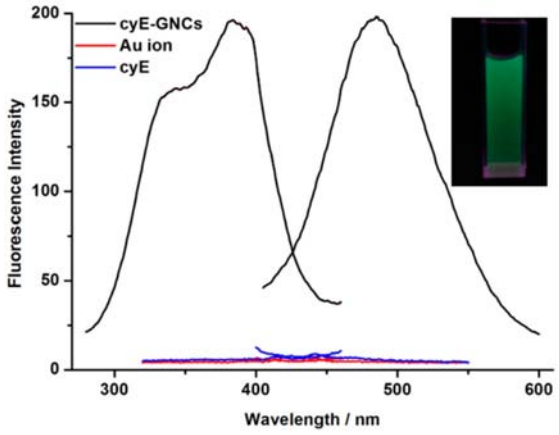

Figure 5. Fluorescence excitation and emission spectra of RGD-GNCs (black curves, excitation at 385 nm and emission at 485 nm), Au ions (red curves), and cyclic RGD peptides (blue curves). The inset shows a photograph of RGD-GNCs under a UV light source emitting 365 nm light.

Figure 6 provides the Fourier transform infrared spectroscopy (FTIR) spectra of the cyclic RGD peptides (a) and the RGD-GNCs (b). The IR absorption peaks at 1666 cm^{-1} (amide I, carbonyl stretch vibration) and 1385 cm^{-1} (amide III, C−N stretch vibration),[23] which are representatives of peptides, were also found in the spectrum of the GNCs, indicating the successful binding of cyclic peptide molecules to the GNCs.

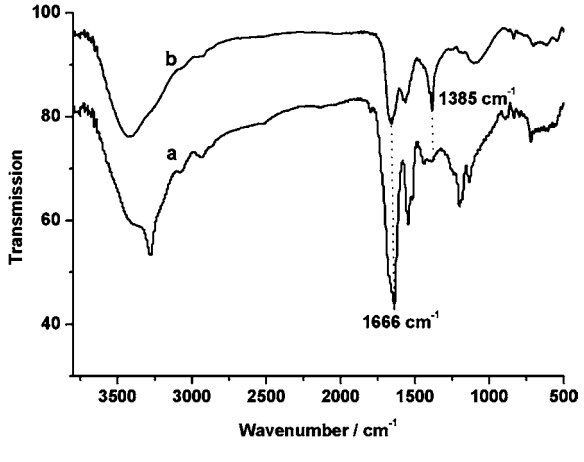

Figure 6. FTIR spectra of cyclic RGD peptide (a) and RGD-GNCs (b). The spectra between them are enlarged 10 units for the contrast distinctly.

X-ray photoelectron spectroscopy (XPS) was used to determine the in-depth chemical state of gold nanoclusters. As shown in Figure 7, there were two peaks located at the

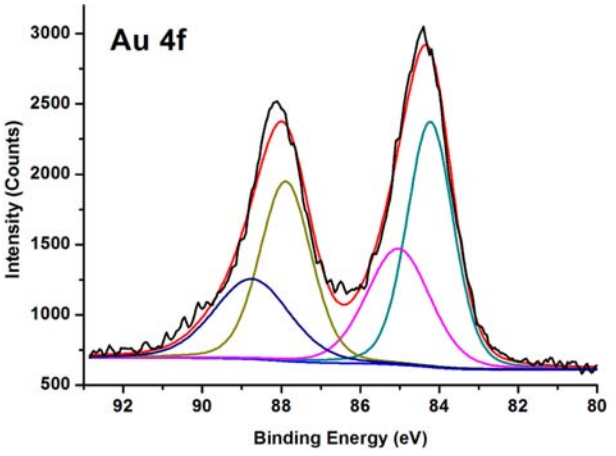

Figure 7. XPS spectrum of the Au 4f of the RGD-GNCs (the original spectra - black; the fitted result - red). The Au 4f7/2 binding energy was deconvoluted into two components, which showed peaks at 84.2 eV (Au(0) - green) and 85.1 eV (Au(I) - purple).

binding energies of around 84.4 and 88.2 eV, which is consistent with the emission of 4f 7/2 and 4f 5/2 photoelectrons from Au 0.[24] The best fit spectrum of Au 4f 7/2 could be deconvoluted into two distinct components (green and purple curves) centered at binding energies of 84.2 and 85.1 eV, which could be assigned to Au(0) and Au(I), respectively.[25−29] There was a certain amount of Au(I) (~39%) present on the surface of the Au core, which helped to stabilize the GNCs.[9] These results indicated that the formation of $[Au(I)Cl_2]^-$ ions could be bound to the pronated peptides by the gold−nitrogen interaction.[30−32]

The MALDI-TOF mass measurement in Figure 8 shows that the green GNCs contained 13 gold atoms (m/z = 2561), which was consistent with the published reference.[33,34] The lifetime of GNCs was also collected on a combined fluorescence lifetime

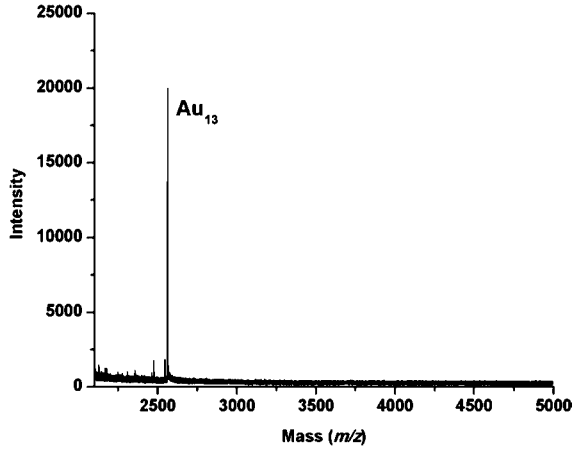

Figure 8. MALDI-TOF MS of RGD-GNCs recorded in the positive mode.

DOI: 10.1021/bc500505c
Bioconjugate Chem. 2015, 26, 243−249

and steady state spectrometer (Figure 9). The decay curves of the emission intensities were fitted with a double exponential

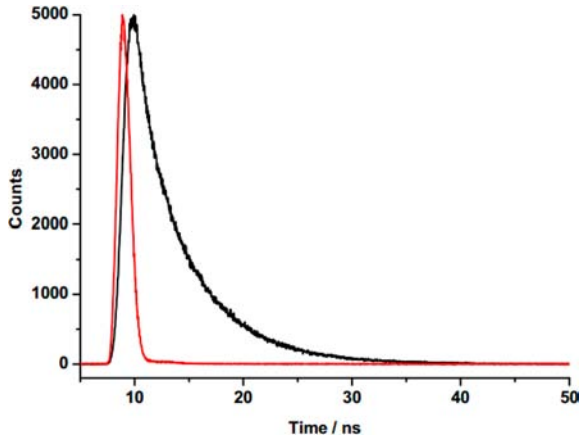

Figure 9. Luminescence lifetime of the RGD-GNCs (black -the fitted curve, red - instrument response function (IRF) curve).

function model, which showed that RGD-GNCs had an average lifetime of 5 ns (87%). The quantum yield (QY) of Au13 clusters was measured to be 4.05%, using quinine sulfate as the reference.

To determine the fluorescence stability of RGD−GNCs, we measured their fluorescence spectra at same concentrations while the GNCs were dispersed in DMEM medium, PBS buffer solution, and water, respectively. As shown in Figure 10, the

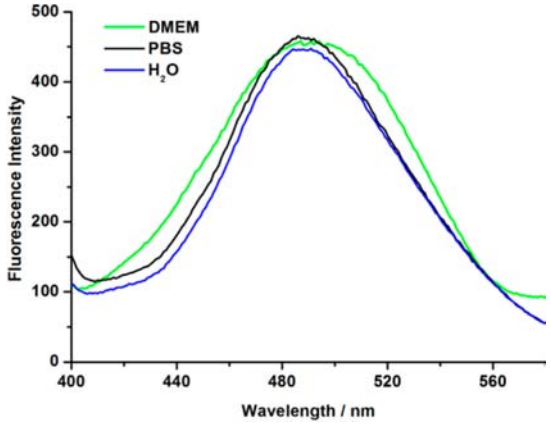

Figure 10. Fluorescence spectra of the GNCs dispersed in DMEM medium (green curve), PBS buffer solution (black curve), and water (black curve).

fluorescence intensities and the emission spectra did not change obviously, indicating that the synthesized RGD−GNCs possessed good fluorescence stability in physiological status.

The A375 cell line that overexpresses the integrin $\alpha_v\beta_3$ was selected as the test group and the MCF-7 breast cancer cell that expresses the integrin $\alpha_v\beta_3$ at a very low level was set as the control group. The cytotoxicity of the RGD-GNCs was measured by the MTT assay (Supporting Information Figure S6). The viability of A375 and MCF-7 remained over 63% after incubation with 10 μg/mL of RGD-GNCs for 1 h as compared to the control groups, which were incubated with an equal amount of PBS buffer and the viability of the control groups was set as 100%. The results illustrated that the prepared GNCs had low cytotoxicity and were suitable for tumor imaging.

The uptake of GNCs (10 μg/mL) by both cell lines after 1.0 h of incubation was assessed by a two photon confocal fluorescence microscopy with a 405 nm laser (consistent for all test conditions). Figure 11(1) clearly demonstrated the entrance condition of RGD-GNCs in both cells, and A_2 exhibited a strong green fluorescence, which meant that there were large amounts of RGD-GNCs in A375 cells. However, there was only background in MCF-7 cells (B_2), indicating that small amounts of GNCs had entered the MCF-7 cells. The entry process relies on the recognition between the $\alpha_v\beta_3$ integrin and RGD peptides conjugated on the surface of prepared GNCs, which was compatible with the entrance mechanism.

Quantitative determinations were carried out to compare the amounts of RGD−GNCs taken up by A375 and MCF-7 cells. In Figure 11(2), we selected 30 μm in both cells and presented the corresponding intensity data in the form of spectra in Figure 11(3). Consistent with the fluorescence imaging images, we can find that the peak area of A375 cells (457.65) was much larger than that of MCF-7 cells (54.7), indicating that there were much more GNCs entered in A375 cells.

In the competitive inhibition assay, the A375 cells were preincubated with free cyclic RGD peptides (0.64 mM, 20 uL), washed with PBS buffer solution, and then incubated with RGD-GNCs (10 μg/mL) for 0.5 h (Figure 12B) while the control group was just incubated with RGD-GNCs for 0.5 h (Figure 12A). Compared with A and B, one can see that there was almost no fluorescence observed in B_2; however, A_2 showed a strong fluorescence although A375 cells were incubated with RGD-GNCs for only 0.5 h. The results show that free peptides could compete for binding to the $\alpha_v\beta_3$ integrin on the cell membrane, which blocked the internalization of RGD-GNCs with the $\alpha_v\beta_3$ overexpressed in A375 cells. As a result, it will reduce the availability of the $\alpha_v\beta_3$ integrin for RGD-GNCs. This indicated that the cyclic RGD peptides conjugated on the surface of GNCs facilitated the uptake by A375 cells through receptor-mediated endocytosis.

CONCLUSION

We have successfully developed a rapid and one-step method to synthesize cyclic RGD conjugated GNCs, which only needs 15 min at room temperature. We made the cyclic RGD molecules play triple roles as reducing, stabilizing, and targeting agents in the one-step synthesis. The prepared GNCs possess good biocompatibility and fluorescence stability. The results of fluorescent imaging and the competitive inhibition assay proved that the receptor-mediated cell internalization can efficiently facilitate delivery of the GNCs into A375 cancer cells, and the specific targeting activity of the peptides on our RGD−GNCs were not influenced noticeably after the peptides acted as a reducing reagent. The results demonstrated that it is also a green synthesis method for reducing costs, simplifying the synthetic process, and shortening the reaction time significantly.

EXPERIMENTAL PROCEDURES

Chemicals. All the chemicals were of reagent grade. $HAuCl_4{\cdot}3H_2O$ was purchased from Sinopharm Chemical Reagent Co., Ltd. (Shanghai, China). The cyclic arginine-glycine-aspartate-tyrosine-glutamic acid (c(RGDyE)), cyclic

DOI: 10.1021/bc500505c
Bioconjugate Chem. 2015, 26, 243−249

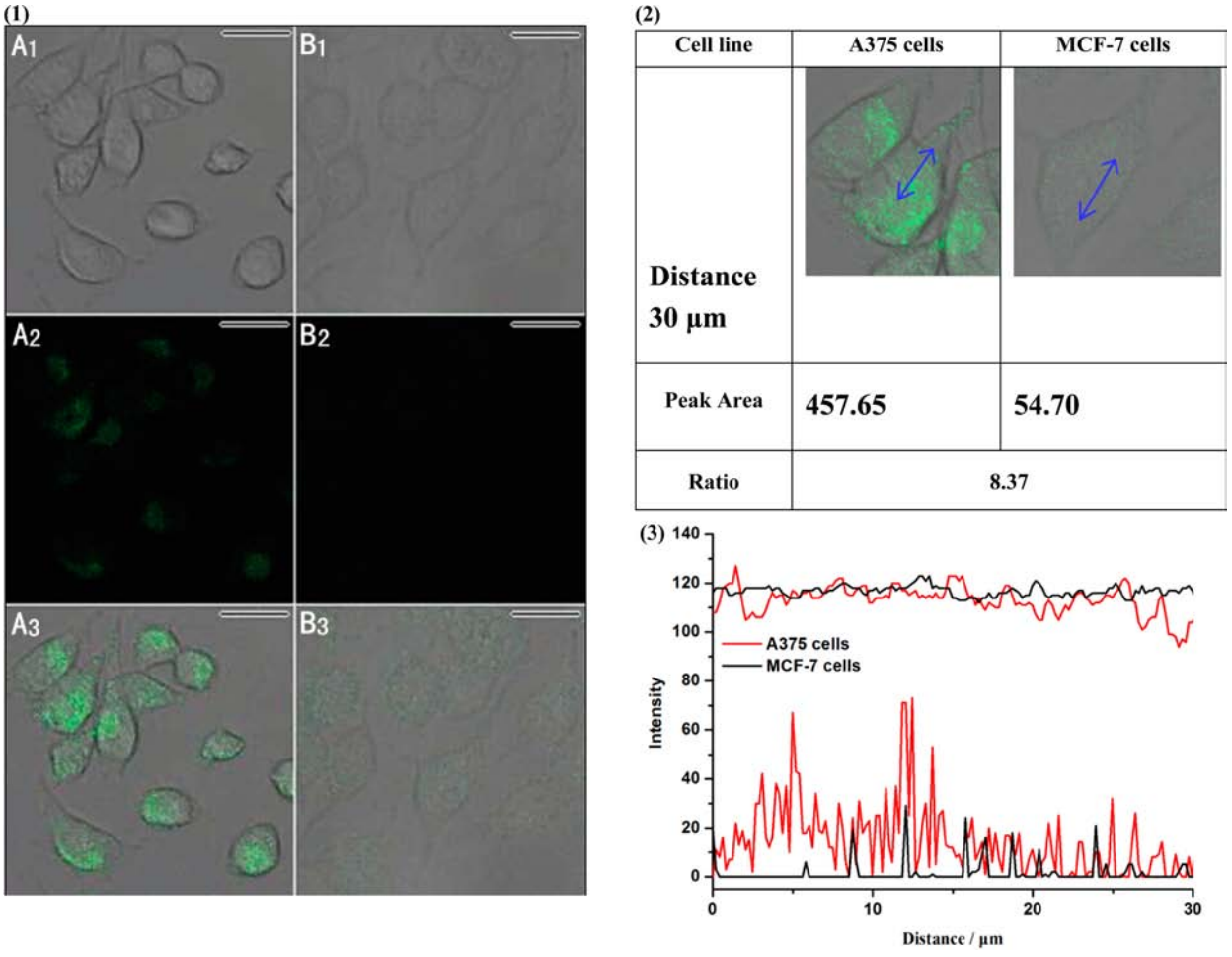

Figure 11. (1) Confocal fluorescence images of A375 cells (A) and MCF-7 cells (B). A_3 and B_3 are the overlapping images of bright (A_1, B_1) and fluorescent images (A_2, B_2). All of the scale bars are 20 μm. (2) Comparison of RGD−GNCs taken up by A375 and MCF-7 cells. The peak area represents the integral of the fluoresence data of the selected distance. (3) Spectra of the fluoresence intensity of the selected distance (30 μm). The top spectra represent the brightness of the bright field pictures, and the lower ones represent the fluoresence intensity.

arginine-glycine-aspartate-tyrosine-cysteic acid (c(RGDyC)), cyclic arginine-glycine-aspartate-phenylalanine-cysteic acid (c-(RGDfC)), and cyclic arginine-glycine-aspartate-phenylalanine-valine (c(RGDfV)) were purchased from China Peptides Co., Ltd. (Shanghai, China). The linear arginine-glycine-aspartic acid (RGD) were purchased from Biotech Bioscience and Technology Co., Ltd. (Shanghai, China). Sodium hydroxide was purchased from Damao Chemical (Tianjin, China). The melanoma A375 and the MCF-7 cell lines were purchased from Shanghai Institutes For Biological Sciences, Chinese Academy of Sciences. Dulbecco Modified Eagle's Medium (DMEM) was purchased from HyClone Technologies. The MTT Cell Proliferation and Cytotoxicity Assay Kit was supplied by KeyGENE BioTECH (Nanjing, China). Ultra pure water of 18.0 MΩ was used for all experiments.

Preparation of RGD-GNCs. For the synthesis of c-(RGDyE) conjugated GNCs, 35 μL of 1 M sodium hydroxide was first added into the aqueous solution of the c(RGDyE) peptides (0.64 mM, 1.0 mL) under magnetic stirring to fulfill the reducing ability of the peptides. Then, Au ion solution (1.20 mM, 1.0 mL) was added into the aqueous solution of the peptides. The reactions continued for 15 min at room temperature, and the color of the solution changed from light yellow to light red. The red color is attributed to the colloidal gold nanoparticles because the GNCs were nearly colorless to the naked eye. The solution containing peptide-conjugated GNCs was purified by centrifugation at 20 000 rpm for 1 h. After removing the bottom precipitate, the supernatant was dialyzed for 12 h to remove excess reactants.

In the following experiments, all the conditions were fixed as above except for the experiments for conditional optimization.

UV−visible, FTIR, Fluorescence, TEM, and XPS Spectroscopic Studies. UV 3150 Spectrophotometer (Shimadzu, Japan) was used to measure the UV−visible spectra of the RGD-GNCs using 1 cm path length quartz cuvettes with 0.1 nm resolution. Fourier transform infrared (FTIR) spectrum of the RGD peptides and RGD−GNCs were obtained from a Nicolet Avatar FTIR model 330 spectrometer (Thermo, America) with the range from 500 to 3800 cm^{-1}. The fluorescence spectra were obtained on a RF-5301 Fluorospectrophotometer (Shimadzu, Japan) with the excited and emissive slit of 5 nm. The samples for transmission electron microscope (TEM) were prepared by dropping the RGD−GNCs solution onto a carbon-coated copper grid, drying at room temperature, and then characterizing by a TEM (JEM-2010HR, JEOL, Japan) operated at an accelerating voltage of 200 kV. The surface compositions of RGD−GNCs were investigated by an ESCALab250 X-ray photoelectron spectroscopy (XPS) (Thermo, America).

DOI: 10.1021/bc500505c
Bioconjugate Chem. 2015, 26, 243−249

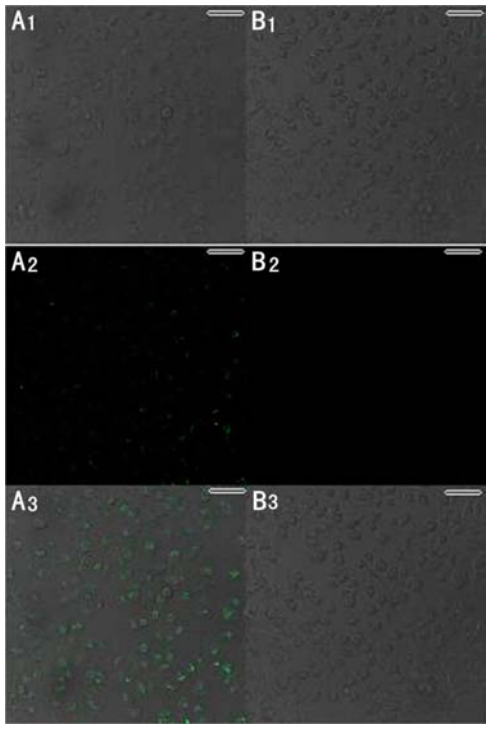

Figure 12. Confocal fluorescence images of competitive inhibition assay of A375 cells. A represents that A375 cells were just incubated with RGD-GNCs; B represents that A375 cells were preincubated with free cyclic RGD peptides and then incubated with RGD-GNCs. A_3 and B_3 are the overlapping images of bright (A_1, B_1) and fluorescent images (A_2, B_2), respectively. All of the scale bars are 50 μm.

ICP Analysis. Inductively coupled plasma-atomic emission spectrometry (ICP-AES, IRIS, TJA, USA) was used to determine the quantities of Au in the RGD-GNCs. The RGD-GNCs were digested in hot HNO_3 (65%), and then diluted with dilute aqua regia to a final volume of 10.0 mL for ICP-AES measurements. The calibration solutions were prepared from a stock standard solution supplied by SPEX Certiprep and the concentration range is from 0.0 to 10.0 ppm Au. Three replicate measurements were made for each sample.

MALDI-TOF MS Measurement. The MALDI-TOF mass measurement of the prepared RGD−GNCs was determined on a Bruker ultrafleXtreme MALDI-TOF/TOF system (Bruker Daltonics, America) in positive mode with 2,5-dihydroxy benzoic acid as the matrix.

Cell Culture. The A375 and MCF-7 cells were cultured in DMEM medium supplemented with 10% FBS in a humidified 5% CO_2 balanced air incubator at 37 °C for 24 h. The cells were collected and implanted onto the confocal dishes, and the culturing was continued for 1 day.

Cytotoxicity Assay. Equal amounts of A375 and MCF-7 cells (5×10^3 cells/well) in the exponential phase were added to each well of two 96-well plates and incubated for 24 h, respectively. Then the RGD−GNCs of concentrations 10, 5, 2.5, 1.25, and 0.625 μg/mL were added to each well of two 96-well plates and incubated for 1 h at 37 °C, respectively. Cells without addition of the RGD−GNCs were used as the control group and the viability was set as 100%. A solution of 50 μL of the MTT was added to each of the wells and incubated for 1 h at 37 °C. The OD values at 450 nm were measured with a microplate reader (Victor X5, PerkinElmer). Three wells for each concentration were set up and the final values were expressed as a percentage of the control.

Imaging GNCs in A375 and MCF-7 Cells. The RGD−GNCs of 10 μg/mL were added into a confocal dish and incubated with both cells for 1 h. Subsequently, these cells were rinsed with phosphate buffer solution (PBS) for three times to remove free and physically absorbed GNCs. Then these cells were imaged by a two photon confocal fluorescence microscopy (Zeisgs-LSM 710, laser: 405 nm) at 400× magnification.

Competitive Inhibition Assay. The competitive inhibition control experiments of A375 cells was also performed by culturing cells with free cRGDyE peptides (20 μL, 0.64 mM) primarily and then with the RGD−GNCs (10 μg/mL) for 0.5 h. Finally, the cells was washed with PBS buffer, and then examined under the laser scanning confocal fluorescence microscope (Leica, TCS-SP5, laser: 405 nm) at 400× magnification.

■ ASSOCIATED CONTENT

Supporting Information

Fluorescence spectra of the optimized conditions of the additional order of raw materials, the ratio of c(RGDyE)/$HAuCl_4$, the amount of sodium hydroxide, the reaction time and temperature, MTT results. This material is available free of charge via the Internet at http://pubs.acs.org.

■ AUTHOR INFORMATION

Corresponding Author

*E-mail: cesgf@mail.sysu.edu.cn. Fax: +86 20 841122 45. Tel: +86 20 34022092.

Notes

The authors declare no competing financial interest.

■ ACKNOWLEDGMENTS

This work was supported by the National Natural Science Foundation of China (20875106), Guangdong Natural Science Found Committee (9151027501000003), and State Key Laboratory of Chemo/Biosensing and Chemometrics, Hunan University (4299001).

■ REFERENCES

(1) Kuphal, S., Bauer, R., and Bosserhoff, A. K. (2005) Integrin signaling in malignant melanoma. *Cancer Metastasis Rev. 24*, 195−222.

(2) Beck, V., Herold, H., Benge, A., Luber, B., Hutzler, P., Tschesche, H., Kessler, H., Schmitt, M., Geppert, H. G., and Reuning, U. (2005) ADAM15 decreases integrin $\alpha_v\beta_3$/vitronectin-mediated ovarian cancer cell adhesion and motility in an RGD-dependent fashion. *Int. J. Biochem. Cell Biol. 37*, 590−603.

(3) Ding, Q., Stewart, J., Olman, M. A., Klobe, M. R., and Gladson, C. L. (2003) The pattern of enhancement of Src kinase activity on platelet-derived growth factor stimulation of glioblastoma cells is affected by the integrin engaged. *J. Biol. Chem. 278*, 39882−39891.

(4) Davis, D. H., Giannoulis, C. S., Johnson, R. W., and Desai, T. A. (2002) Immobilization of RGD to <111> silicon surfaces for enhanced cell adhesion and proliferation. *Biomaterials 23*, 4019−4027.

(5) He, H., Sun, X., Wang, X. J., Sun, Y. W., and Xu, H. L. (2014) Cyclic arginyl-glycyl-aspartic acid (RGD) peptide-induced synthesis of uniform and stable one-dimensional CdTe nanostructures in aqueous solution. *RSC Adv. 4*, 11794−11797.

(6) He, H., Feng, M., Hu, J., Chen, C., Wang, J., Wang, X., Xu, H., and Lu, J. R. (2012) Designed short RGD peptides for one-pot aqueous synthesis of integrin-binding CdTe and CdZnTe quantum dots. *ACS Appl. Mater. Interfaces. 4*, 6362−6370.

DOI: 10.1021/bc500505c
Bioconjugate Chem. 2015, 26, 243−249

(7) Arosio, D., Manzoni, L., Araldi, M. V., and Scolastico, C. (2011) Cyclic RGD functionalized gold nanoparticles for tumor targeting. *Bioconjugate Chem. 22*, 664−672.
(8) Scari, G., Porta, F., Fascio, U., Avvakumova, S., and Santo, V. D. (2012) Gold nanoparticles capped by a GC-containing peptide functionalized with an RGD motif for integrin targeting. *Bioconjugate Chem. 23*, 340−349.
(9) Kim, Y. H., Jeon, J., Hong, S. H., Rhim, W. K., Lee, Y. S., and Youn, H. (2011) Tumor Targeting and imaging using cyclic RGD-pegylated gold nanoparticle probes with directly conjugated iodine-125. *Small 14*, 2052−2060.
(10) Yin, H. Q., Mai, D. S., Gan, F., and Chen, X. J. (2014) One-step synthesis of linear and cyclic RGD conjugated gold nanoparticles for tumour targeting and imaging. *RSC Adv. 4*, 9078−9085.
(11) Das, B., Fernandez, F., John, A., and Sharma, C. P. (2012) Cyclic RGD peptide conjugated trypsin etched gold quantum clusters: novel biolabeling agents for stem cell imaging. *Journal of Stem Cells 7*, 189−199.
(12) Shang, L., Dong, S. J., and Nienhaus, G. U. (2011) Ultra-small fluorescent metal nanoclusters: Synthesis and biological applications. *Nano Today 6*, 401−418.
(13) Xie, J. P., Zheng, Y. G., and Jackie, Y. Y. (2009) Protein-directed synthesis of highly fluorescent gold nanoclusters. *J. Am. Chem. Soc. 131*, 888−889.
(14) Tan, Y. N., Lee, J. Y., and Wang, D. I. C. (2010) Uncovering the design rules for peptide synthesis of metal nanoparticles. *J. Am. Chem. Soc. 132*, 5677−5686.
(15) Chen, T. H., and Tseng, W. L. (2012) (Lysozyme Type VI)-stabilized Au_8 clusters: synthesis mechanism and application for sensing of glutathione in a single drop of blood. *small 8*, 1912−1919.
(16) Liu, C. L., Wu, H. T., Hsiao, Y. H., Lai, C. W., Shih, C. W., Peng, Y. K., Tang, K. C., Chang, H. W., Chien, Y. C., Hsiao, J. K., Cheng, J. T., and Chou, P. T. (2011) Insulin-directed synthesis of fluorescent gold nanoclusters: preservation of insulin bioactivity and versatility in cell imaging. *Angew. Chem., Int. Ed. 50*, 7056−7060.
(17) Sun, C. J., Yang, H., Yuan, Y., Tian, X., Wang, L. M., Guo, Y., Xu, L., Lei, J. L., Gao, N., Anderson, G. J., Liang, X. J., Chen, C., Zhao, Y., and Nie, G. (2011) Controlling assembly of paired gold clusters within apoferritin nanoreactor for in vivo kidney targeting and biomedical imaging. *J. Am. Chem. Soc. 133* (22), 8617−8624.
(18) Wang, Y. L., Cui, Y. Y., Zhao, Y. L., Liu, R., Sun, Z. P., Li, W., and Gao, X. Y. (2012) Bifunctional peptides that precisely biomineralize Au clusters and specifically stain cell nuclei. *Chem. Commun. 48*, 871−873.
(19) Ji, X. H., Song, X. G., Li, J., Jun, Y. B., Yang, W. S., and Peng, X. G. (2007) Size control of gold nanocrystals in citrate reduction: the third role of citrate. *J. Am. Chem. Soc. 129*, 13939−13948.
(20) Lippard, S. J., and Berg, J. M. (1994) *Principles of Bioinorganic Chemistry*, University Science Books, Mill Valley, CA.
(21) Li, G. P., Li, D., Zhang, L. X., Zhai, J. F., and Wang, E. K. (2009) One-step synthesis of folic acid protected gold nanoparticles and their receptor-mediated intracellular uptake. *Chem.—Eur. J. 15*, 9868−9873.
(22) Ayala, I. P., Sacksteder, C. A., and Barry, B. A. (2003) Redox-active tyrosine residues: role for the peptide bond in electron transfer. *J. Am. Chem. Soc. 125*, 7536−7538.
(23) Schweitzer-Stenner, R., Eker, F., Huang, Q., Griebenow, K., Mroz, P. A., and Kozlowski, P. M. (2002) Structure analysis of dipeptides in water by exploring and utilizing the structural sensitivity of amide III by polarized visible Raman, FTIR-spectroscopy and DFT based normal coordinate analysis. *J. Phys. Chem. B 106*, 4294−4304.
(24) Zhao, W. A., Gonzaga, F., Li, Y. F., and Brook, M. A. (2007) Highly stabilized nucleotide-capped small gold nanoparticles with tunable size. *Adv. Mater. 19*, 1766−1771.
(25) Zhang, Z. Y., Xu, L. J., Li, H. X., and Kong, J. L. (2013) Wavelength-tunable luminescent gold nanoparticles generated by cooperation ligand exchange and their potential application in cellular imaging. *RSC Adv. 3*, 59−63.
(26) Chaudhari, K., Xavier, P. L., and Pradeep, T. (2011) Understanding the evolution of luminescent gold quantum clusters in protein templates. *ACS Nano 5*, 8816−8827.
(27) Cai, Y. Q., Yan, L., Liu, G. Y., Yuan, H. Y., and Xiao, D. (2013) In-situ synthesis of fluorescent gold nanoclusters with electrospun fibrous membrane and application on Hg (II) sensing. *Biosens. Bioelectron. 41*, 875−879.
(28) Guevel, X. L., Daum, N., and Schneider, M. (2011) Synthesis and characterization of human transferrin-stabilized gold nanoclusters. *Nanotechnology 22*, 275103.
(29) Tu, X. J., Chen, W. B., and Guo, X. Q. (2011) Facile one-pot synthesis of near-infrared luminescent gold nanoparticles for sensing copper (II). *Nanotechnology 22*, 095701.
(30) Porta, F., Krpetic, Z., Prati, L., Gaiassi, A., and Scari, G. (2008) Gold-ligand interaction studies of water-soluble aminoalcohol capped gold nanoparticles by NMR. *Langmuir 24*, 7061−7064.
(31) Kumar, A., Mandal, S., Selvakannan, P. R., Pasricha, R., Mandale, A. B., and Sastry, M. (2003) Investigation into the interaction between surface-bound alkylamines and gold nanoparticles. *Langmuir 19*, 6277−6282.
(32) Newman, J. D. S., and Blanchard, G. J. (2006) Formation of gold nanoparticles using amine reducing agents. *Langmuir 22*, 5882−5887.
(33) Venkatesh, V., Shukla, A., Sivakumar, S., and Verma, S. (2014) Purine-stabilized green fluorescent gold nanoclusters for cell nuclei imaging applications. *ACS Appl. Mater. Interfaces 6*, 2185−2191.
(34) Zheng, J., Zhang, C. W., and Dickson, R. M. (2004) Highly fluorescent, water-soluble, size-tunable gold quantum dots. *Phys. Rev. Lett. 93*, 077402.

DOI: 10.1021/bc500505c
Bioconjugate Chem. 2015, 26, 243−249